Epigenetics & Chromatin

RESEARCH Open Access

Function of HP1BP3 as a linker histone is regulated by linker histone chaperones, NPM1 and TAF-I

Miharu Hisaoka[1], Tetsuro Komatsu[2], Takuma Hashimoto[3], Jianhuang Lin[1,4], Yasuyuki Ohkawa[5] and Mitsuru Okuwaki[3*]

Abstract

Background Linker histones constitute a class of proteins that are responsible for the formation of higher-order chromatin structures. Core histones are integral components of nucleosome core particles (NCPs), whereas linker histones bind to linker DNA between NCPs. Heterochromatin protein 1 binding protein 3 (HP1BP3) displays sequence similarity to linker histones, with the exception of the presence of three globular domains in its central region. However, the function of HP1BP3 as a linker histone has not been analyzed previously. The present study aimed to elucidate the function of full-length HP1BP3 as a linker histone variant.

Results The results of biochemical analyses demonstrate that HP1BP3 efficiently binds to NCPs with similar efficiency as linker histones, thereby forming a chromatosome. Notwithstanding the presence of three globular domains, the results suggest that a single HP1BP3 binds to a single NCP under our biochemical assay condition. Moreover, our findings revealed that the NCP binding activity of HP1BP3 is regulated by linker histone chaperones, nucleophosmin (NPM1) and template activating factor-I (TAF-I). The globular domains and the C-terminal disordered region of HP1BP3 are responsible for binding to histone chaperones. Chromatin immunoprecipitation-sequence analyses demonstrated that HP1BP3 exhibited weak preferences for the genomic loci where histone H3 active modification marks were enriched, whereas a linker histone variant, H1.2, showed weak preferences for the genomic loci where histone H3 inactive modification marks were enriched. It is noteworthy that the preferential binding tendencies of HP1BP3 and H1.2 to active and inactive genomic loci, respectively, are diminished upon the knockdown of either NPM1 or TAF-I.

Conclusions Our findings indicate that HP1BP3 functions as a linker histone variant and that the chromatin binding preference of linker histones, including HP1BP3, is regulated by linker histone chaperones.

*Correspondence:
Mitsuru Okuwaki
okuwakim@pharm.kitasato-u.ac.jp
[1]Graduate School of Comprehensive Sciences, University of Tsukuba, 1-1-1 Tennodai, Tsukuba 305- 8575, Japan
[2]Laboratory of Epigenetics and Metabolism, Institute for Molecular and Cellular Regulation, Gunma University, Gunma 371-8512, Japan
[3]Laboratory of Biochemistry, School of Pharmacy and Graduate School of Pharmaceutical Sciences, Kitasato University, 5-9-1 Shirokane, Minato-Ku, Tokyo 108-8641, Japan
[4]PhD Program of Human Biology, School of Integrative and Global Majors, University of Tsukuba, 1-1-1 Tennodai, Tsukuba 305-8575, Japan
[5]Division of Transcriptomics, Medical Institute of Bioregulation, Kyushu University, 3-1-1 Maidashi, Higashi 812-0054, Fukuoka, Japan

Background

Long genomic DNA is folded into chromatin with core histones, histone H2A, H2B, H3, and H4. Assembly and disassembly of nucleosomes at specific genomic loci, or the structural conversion between euchromatin and heterochromatin, play essential roles in turning gene expression on and off. Core histones are major structural proteins of nucleosome core particle (NCP), whereas linker histones are proteins that bind the linker regions between nucleosomes to form compact chromatin structure. Linker histones consist of N- and C-terminal disordered regions and a central globular domain. Recent structural study has demonstrated that the globular domains of linker histones reside on the dyad axis of nucleosome and are a ssociated with both linker DNAs entering in or exiting from the nucleosome [1]. The different nucleosome binding mode of the globular domains has been also reported [2]. The disordered C-terminal region stabilizes the binding of linker histones with NCPs [3] and the binding of the C-terminal regions to linker DNAs change their orientations [1]. In mammalian somatic cells, 7 linker histone variants, H1.1, H1.2, H1.3, H1.4, H1.5, H1.0, and H1.X, are expressed. Because simultaneous knockout of three linker histone genes causes embryonic lethality [4], linker histones are essential for mice development. However, single knockout of the linker histone variant genes in mice did not show clear phenotype [5], suggesting that these variants play redundant roles in regulating chromatin structure and gene expression, although specific functions of some of the variants are also reported [6].

While core histones are distributed throughout the genome, linker histones are not distributed across the entire genome. Chromatin-immunoprecipitation followed by sequencing (ChIP-Seq) technique is a powerful tool to determine the sites of the genome bound by target proteins. Various ChIP-Seq data have been reported for linker histone variants [7–10]. By obtaining ChIP-Seq data, it is possible to roughly predict the chromatin epigenetic states where the target proteins are located [11]. The epigenetic marks of core histones are useful indicators of chromatin states, with the di- and tri-methylation of histone H3K9 and H3K27 are inactive states and the acetylation of histone H3K27 and methylation of histone H3K4 are indicatives of active states.

Histones are typically comprised of a high proportion of basic amino acids and have been observed to exhibit non-specific binding to DNA or RNA in vitro. In cells, non-specific DNA/RNA binding must be rigorously suppressed. In the event that non-specific DNA/RNA binding of histones is not properly suppressed, it will have a significantly detrimental impact on the functions of DNA and RNA, including processes such as DNA replication, transcription, and translation. The binding of acidic proteins or RNAs to histones has been demonstrated to suppress non-specific DNA binding of histones, thereby facilitating the formation of proper NCPs or NCP-linker histone complexes [12–15]. TAF-I, NAP1, NPM1, NCL, and Prothymosin α have been demonstrated to be associated with linker histones in the cell extracts, and to mediate association and dissociation of linker histones with NCPs [16–19]. Furthermore, our previous findings have demonstrated that TAF-I depletion reduces linker histone dynamics in HeLa cells [16], and analogous outcomes were observed for Prothymosin α [20]. Therefore, it is postulated that these linker histone binding proteins exert a pivotal function in regulating chromatin structure by influencing linker histone dynamics within cells. Nevertheless, the precise functions of these acidic proteins with respect to linker histone chromatin binding remain elusive.

HP1BP3 was initially identified as a binding partner of the heterochromatin protein HP1α, through yeast two-hybrid screening [11]. HP1BP3 exhibits a protein domain composition analogous to that of linker histones except for its three globular domains. Biochemical analyses of the first globular domain alone demonstrated its capacity to associate with NCPs like linker histone H1.2 [21]. It has been documented that mice lacking HP1BP3 exhibit growth retardation at birth [22]. Additionally, it has been demonstrated that HP1BP3 plays a role in microRNA (miRNA) biogenesis by interacting with the miRNA processor complex [23]. These results suggest that although the first globular domain of HP1BP3 binds to NCPs similar as do linker histone H1s, it performs specific functions that are distinct from those of linker histone H1 proteins. Nevertheless, the NCP binding of full-length HP1BP3 to NCPs, as well as the distinct and redundant binding of its three globular domains to NCPs, has yet to be investigated. In this study, we sought to elucidate the chromatin binding properties of HP1BP3 and its distribution along the entire chromatin, with a comparison to those of linker histone variants.

Methods

Structure prediction of the globular domains of HP1BP3

The globular domains of HP1BP3, G1 (amino acids 156–233), G2 (amino acids 254–331), and G3 (amino acids 342–414), and those of H1.0 (amino acids 28–98) and H1.2 (amino acids 35–110) were aligned by Clastal W (https://www.genome.jp/tools-bin/clustalw) with default parameter settings. The structures of the globular domains were predicted by AlphaFold 3 [24]. As a reference of the globular domain, the solution structure of the globular domain of H1.0 deposited on the protein data base (PDB) was used (PDB: 6HQ1). The predicted structures and the reference structure were superimposed by PyMol ver. 3.0.4. The template modeling score

(TM-score), representing a metric of the topological similarity of protein structures, was calculated using TM-align [25] (https://zhanggroup.org/TM-align/).

Plasmid construction

HP1BP3 cDNA (UniPort ID: Q5SSJ5) was prepared by PCR (KOD plus-Neo, Toyobo) using HeLa cell cDNA as a template and a primer set, 5'-GAGGATATCCATATG GCGACTGATACGTCTCA-3' and 5'-AGCTCTCGAGT TACTTTTTCACTCTGAAAG-3'. The amplified cDNA was digested with EcoR V and Xho I and subcloned into the same sites of pcDNA3.1-Flag vector. To construct HP1BP3ΔG12, HP1BP3ΔG13, HP1BP3ΔG23 cDNAs, HP1BP3ΔG1, HP1BP3ΔG2, and HP1BP3ΔG3 cDNAs were first amplified by 2-step PCR using primer sets, 5'-T TCTGGATTTCTGAGGCGGTGTTTGTTTCTGGGC CC-3' and 5'-CCAGAAACAAACACCGCCTCAGAAA TCCAGAAACAG-3', 5'-CTGATTTCTTCAGCTGTTC TGGATCCACTGCAGAGC-3' and 5'-TGCAGTGGATC CAGAACAGCTGAAGAAATCAGGGG, and 5'-AGGG AAAACAGAGCTGCAGGCTTCCACCAAGCAGG-3' and 5'-GCTTGGTGGAAGCCTGCAGCTCTGTTTTC CCTATTATC-3', respectively. For PCR amplification of first PCR, vector primers for pcDNA3.1 and pcDNA3.1-Flag-HP1BP3 as a template were used. To prepare HP1BP3ΔG12, HP1BP3ΔG23, and HP1BP3ΔG13, the same PCR reactions were performed using HP1BP3ΔG1 or HP1BP3ΔG2 as templates. Similarly, HP1BP3ΔG123 cDNA was prepared from HP1BP3ΔG23 as a template and a primer set for HP1BP3ΔG1 preparation. The cDNA was cloned into EcoR V and Xho I-digested pcDNA3.1-Flag vector. To construct pEGFP-C1-Flag-HP1BP3, Flag-HP1BP3 cDNA was cut out from pcDNA3.1-Flag vector with Kpn I and Apa I and subcloned into the same sites of pEGFP-C1 vector. pGEX2T-TAF-Iβ and pGEX2T-Flag-NPM1 were previously described [15, 16]. The Widom 601 sequence [26] (250 bp) was amplified by PCR using 5'-AAAGCATGATTCTTCACACC-3' and 5'-CACTATC CGACTGGCACCGG-3'.

Cell growth, FRAP assay, and immunofluorescence

HeLa cells, U2OS cells, and 293T cells were grown in DMEM containing 10% FBS and antibiotics (streptomycin and penicillin). Mouse embryonic fibroblast cells (MEF) lacking *p53* (referred to as control MEF cells) and both *p53* and *NPM1* genes (referred to as NPM1 KO MEF cells) were obtained from Dr. E. Colombo and were maintained in DMEM containing 10% FBS and antibiotics [27]. For FRAP assay with HeLa cells, control siRNA (Thermo Fisher Scientific, 12935200), NPM1 siRNA [28], TAF-I siRNA [16] were transfected by Lipofectamine RNAiMAX (Life Technologies) in U2OS cells, and the cells were incubated for 24 h. Then the cells were re-spread in 3.5 cm glass-based dishes (IWAKI glass) and pEGFP-C1-Flag-HP1BP3 was transiently transfected by Gene Juice (Merck Milipore). The cells were washed with PBS 24 h post plasmid transfection and incubated for an additional 24 h. FRAP assays were performed 72–80 h post siRNA transfection using LSM5 confocal microscope (Zeiss microscopy) as described previously [17]. Similarly, control and NPM1 KO MEF cells were transiently transfected with pEGFP-Flag-HP1BP3 and FRAP assays were conducted as above.

Protein expression and purification

Flag-tagged HP1BP3 and its mutants were expressed in 293T cells and purified with Flag-M2 agarose beads (SIGMA Aldrich). 293T cells expressing Flag-HP1BP3 proteins were suspended in the buffer A (20 mM Tris pH7.9, 0.1% Triton X-100, and 0.1 mM PMSF) containing 50 mM NaCl. The NaCl concentration was adjusted to 400 mM and incubated on ice for 30 min. The extracts were centrifuged at 15,000 rpm for 10 min and the supernatants were recovered. NaCl concentration was diluted to 200 mM by adding buffer A, followed by incubation with Flag-M2 agarose beads (SIGMA Aldrich) for 2 h at 4 °C. The beads were then extensively washed with buffer A containing 400 mM NaCl. The bound Flag-tagged proteins were eluted with buffer H (20 mM Hepes pH7.9, 50 mM NaCl, 10% glycerol, and 0.1 mM PMSF) containing 0.1 mg/ml flag peptide (SIGMA Aldrich). The concentration of the purified proteins was estimated by CBB-stained bands on SDS-PAGE using BSA as a standard. GST-TAF-Iβ and GST-NPM1 were expressed in E. coli and purified as described [17].

Preparation of NCPs and binding assay

NCPs were assembled on 196 bp-long 5 S rDNA sequence and 250 bp-long Widom601 nucleosome positioning sequence with recombinant core histones. Preparation of core histones and NCPs were previously described [17]. NCPs were purified by 15–30% glycerol density gradient and the concentration (DNA) was estimated by band intensity relative to the same DNA separated by PAGE with known concentration as a standard. In the standard NCP-HP1BP3 binding assay, NCPs (0.1 pmole of DNA) were incubated at 37 °C for 30 min in the presence of 0.1 mg/ml BSA and separated by 6% native polyacrylamide gel containing 0.5×Tris-Borate EDTA (TBE). The DNA was visualized by Gel Red staining. For MNase digestion assay, after incubation with or without HP1BP3, the mixture was supplemented with 3 mM $CaCl_2$ followed by MNase digestion at 30 °C. DNA extracted by phenol-chloroform and precipitated with ethanol was separated by native 6% PAGE and visualized by Gel Red staining.

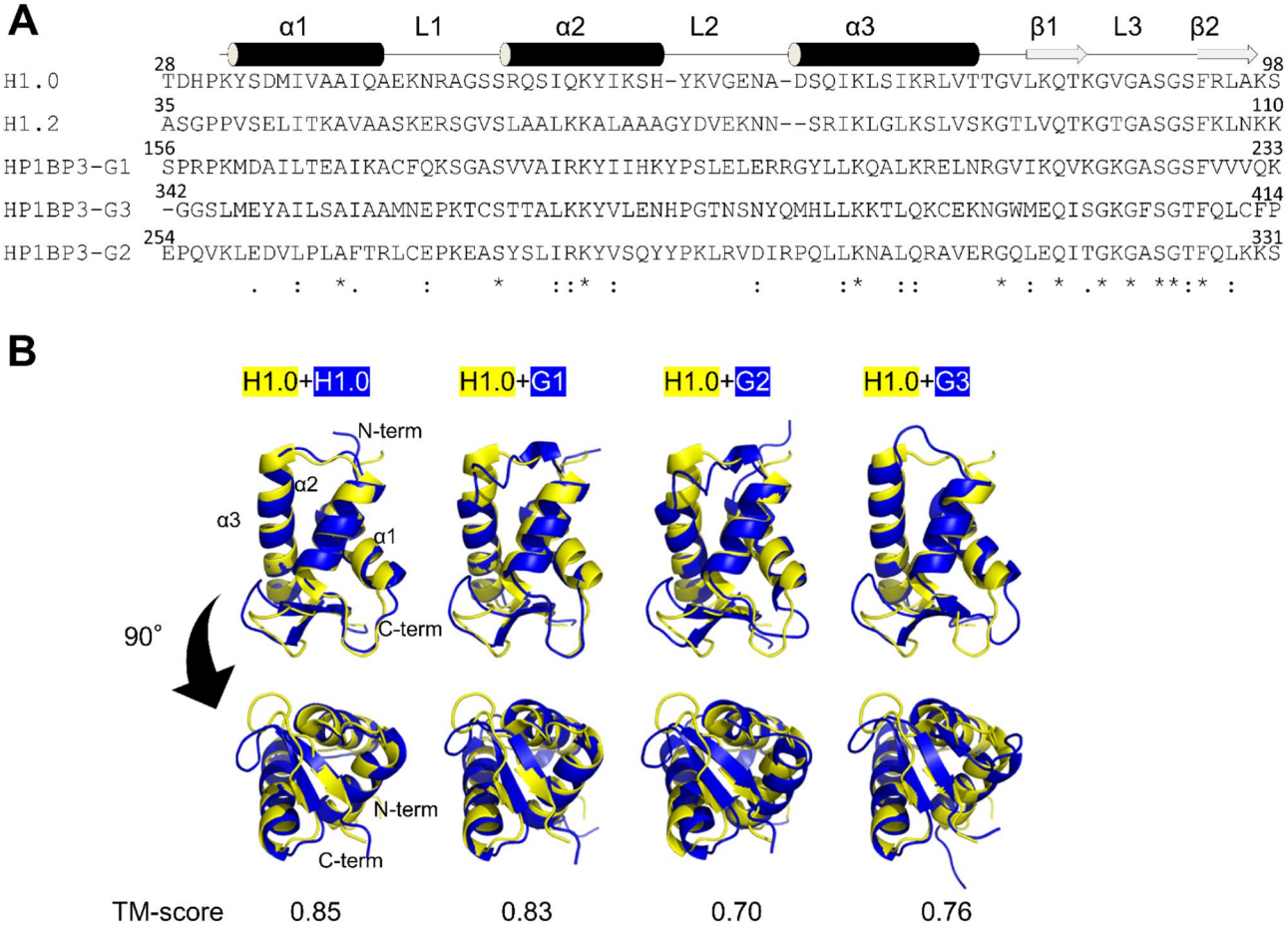

Fig. 1 The globular domains of HP1BP3 show similarity to that of canonical linker histones. (**A**) Alignment of the globular domains of linker histones and HP1BP3. The globular domains of H1.0 (amino acids 28–98) and H1.2 (amino acids 35–110), and HP1BP3 G1 (amino acids 156–233), G2 (amino acids 254–331), and G3 (amino acids 342–414) are aligned by Clastal W (https://www.genome.jp/tools-bin/clustalw) with default parameter settings. The positions of three α helices (α1, α2, and α3), two β sheets (β1 and β2), and linkers (L1, L2, and L3) are represented based on the solution structure of the globular domain of H1.0 (PDB: 6HQ1). (**B**) Structural prediction of the globular domains of HP1BP3. The predicted structures of the globular domains of H1.0, HP1BP3-G1, HP1BP3-G2, and HP1BP3-G3 (indicated by blue) by AlphaFold3 are superimposed on the solution structure of the globular domain of H1.0 (PDB: 6HQ1, indicated by yellow). Positions of α helices, and the N- and C-terminal ends are shown in the superimposed structure for the globular domain of H1.0. TM-scores are shown at the bottom of the panel

Antibodies used in this study

HP1BP3 antibody was raised in rabbits using HP1BP3 as an antigen. The anti-HP1BP3 antibody was purified from rabbit serum with antigen-immobilized HiTrap NHS-activated column (Cytiva). Antibody for TAF-Iβ (KM1720) was described previously [29]. The following antibodies were commercially available; Flag-tag (SIGMA Aldrich), NPM1 (FC-61991, Thermo Fisher Scientific), NCL (D6, Santacruz Biotechnologies), Actin (H6, Santacruz Biotechnologies), anti-Histone 1.2 (ab4086, Abcam), Anti-UBF (F-9, Santacruz Biotechnologies).

Immunoprecipitation and western blotting

HeLa cell nuclear extracts were prepared by standard methods [30]. The extracts were mixed with an anti-HP1BP3 antibody (2 μg) and incubated at 4 °C for 2 h. Protein A Sepharose Fast Flow (Cytiva) was added and further incubated at 4 °C for 30 m. Then, the beads were washed with buffer A containing 100 mM NaCl and the proteins bound to the beads were eluted with SDS-PAGE sample buffer. The proteins were separated by 10% SDS-PAGE followed by western blotting with antibodies against HP1BP3, NPM1, TAF-Iβ, and NCL.

ChIP-sequence analysis

Exponentially growing HeLa cells treated with control siRNA, NPM1 siRNA, or TAF-Iβ siRNA were fixed with 0.5% formaldehyde for 10 min at 37 °C followed by quenching the reaction by an addition of 0.1 M glycine. The cells were suspended in lysis buffer (50 mM Tris HCL [pH7.9], 10 mM EDTA, and 1% sodium dodecyl sulfate) and lysed on ice for 10 min. The genomic DNAs in the cells were disrupted by extensive sonication to obtain DNA fragments with average length of 200 to 500 base

pairs. The chromatin extracts were incubated with anti-HP1BP3 or histone H1.2 antibodies (1 μg of immune globulin) for overnight at 4 °C and the chromatin complexes containing target proteins were recovered with protein A Sepharose Fast Flow (Cytiva) by incubating at 4 °C for 15 min. The chromatin complexes precipitated by the beads were extensively washed as previously described. DNAs recovered by immunoprecipitation were de-crosslinked and extracted by proteinase K treatment and phenol-chloroform. Then, DNA was precipitated with ethanol and its concentration was examined by nano-drop (Thermo Scientific). The precipitated DNA (50 ng) was used for ChIP-Seq library preparation (ThruPLEX DNA-seq kit, Takara Bio) and subsequent sequencing with the Illumina Hi-seq 1500 system. The data was deposited to Gene Expression Omnibus with the accession number of GSE275436.

Bioinformatic analysis was conducted using indicated tools with default settings unless specified otherwise. Reads were subjected to pre-processing using fastp (Galaxy Version 0.23.2 + galaxy0) and then aligned to the hg38 human genome using Bowtie2 (Galaxy Version 2.5.3 + galaxy1, --very-sensitive). To remove multi-mapped, PCR-duplicated, and mitochondrial reads, samtools was used: samtools sort (Galaxy Version 2.0.5), samtools view (Version 1.18, -e 'rname!= "chrM"' -F 0 × 4 -q 40), samtools fixmate (Version 1.18, -m), and samtools markdup (Galaxy Version 1.15.1 + galaxy2, -r). To generate bigWig files, bamCoverage and bigwigCompare of deepTools (Galaxy Version 3.5.4 + galaxy0) were used for CPM normalization and calculating log2 fold change (log2fc) between two conditions, respectively. Bin sizes of bigWig files were changed using bigwigAverage of deepTools (Galaxy Version 3.5.4 + galaxy0) when necessary. Correlation matrix was generated with multiBigwigSummary (--binSize 1000000) and plotCorrelation (--corMethod spearman) of deepTools. For aggregation plots, bed files for top- and bottom-1000 regions (10-kb window) in a given bigWig file were first generated based on a raw count file from multiBigwigSummary of deepTools (--binSize 10000 --outRawCounts). Then, computeMatrix (reference-point --referencePoint center -b 5000 -a 5000 --binSize 500) and plotProfile (--perGroup) of deepTools were used. Visualization of bigWig data was done on IGV (Integrative Genomics Viewer, version 2.8.7).

Public ChIP-Seq data (bigWig files, fold change over control) for histone modifications in HeLa-S3 cells were obtained from the ENCODE portal (https://www.encodeproject.org): H3K4me3 (ENCFF460QIU), H3K27ac (ENCFF658XKZ), H3K9me3 (ENCFF658AOG), and H3K27me3 (ENCFF186NYC).

Results

HP1BP3 is suggested to contain three globular domains that are similar in sequence to the central regions of the linker histone H1 proteins. Moreover, the first globular domain was demonstrated to interact with nucleosome in a manner analogous to that observed for linker histones [21]. Therefore, it was reasonable to speculate that single HP1BP3 molecules could tether three nucleosomes to form a condensed chromatin structure. To gain insight into the function of the three globular domains of HP1BP3, their amino acid sequences (amino acids 156–233, amino acids 254–331, and amino acids 342–414 for the globular domains, G1, G2, and G3, respectively) were aligned and compared with the globular domains of canonical linker histones, H1.0 and H1.2 (Fig. 1A). Compared to the identity and similarity between canonical linker histones H1.0 and H1.2, those between H1.0 and the globular domains of HP1BP3 are more divergent. However, amino acids in three α helices (α1, α2, and α3), two β sheets (β1 and β2), and linker 3 (L3) of H1.0 are relatively well conserved in the globular domains of HP1BP3. Subsequently, we employed the AlphaFold 3 protein structure prediction tool, which is renowned for its high degree of accuracy [24], using the sequences for the globular domains of H1.0 and HP1BP3 shown in Fig. 1A (Fig. 1B). When the experimental NMR structure (PDB:6HQ1) and the AlphaFold 3 predicted structure of the globular domain of H1.0 were superimposed, overall structural units (three α helices followed by two β sheets) in the two structures overlapped well, with minor variations in the length of two β sheets and the orientation of the linker regions (Fig. 1B, left panel). TM-socre, a metric for the structural similarity of target proteins, was determined to be 0.85. This ensures that the prediction by AlphaFold 3 is accurate. Similarly, the AlphaFold predicted structures of the three globular domains of HP1BP3 (HP1BP3-G1, -G2, and -G3) were superimposed on the experimentally obtained structure of the globular domain of H1.0 (Fig. 1B). The results suggest that all the globular domains of HP1BP3 are folded into the folded structures comprising three α helices and two β sheets. Despite the absence of two β sheets in the NMR structure of the G1 of HP1BP3 [21] (PDB: 2RQP), these β sheets may be formed depending on the experimental condition. Given that the TM-scores calculated from the NMR structure of H1.0 globular domain and each HP1BP3 globular domain were all greater than 0.5, the predicated structures of HP1BP3 globular domains are considered to be similar. From these observations, all the globular domains of HP1BP3 are possible to function as NCP binding domains.

We first investigated whether full-length HP1BP3 binds to nucleosome core particles in vitro. To this end, Flag-tagged HP1BP3 was expressed in 293T cells and

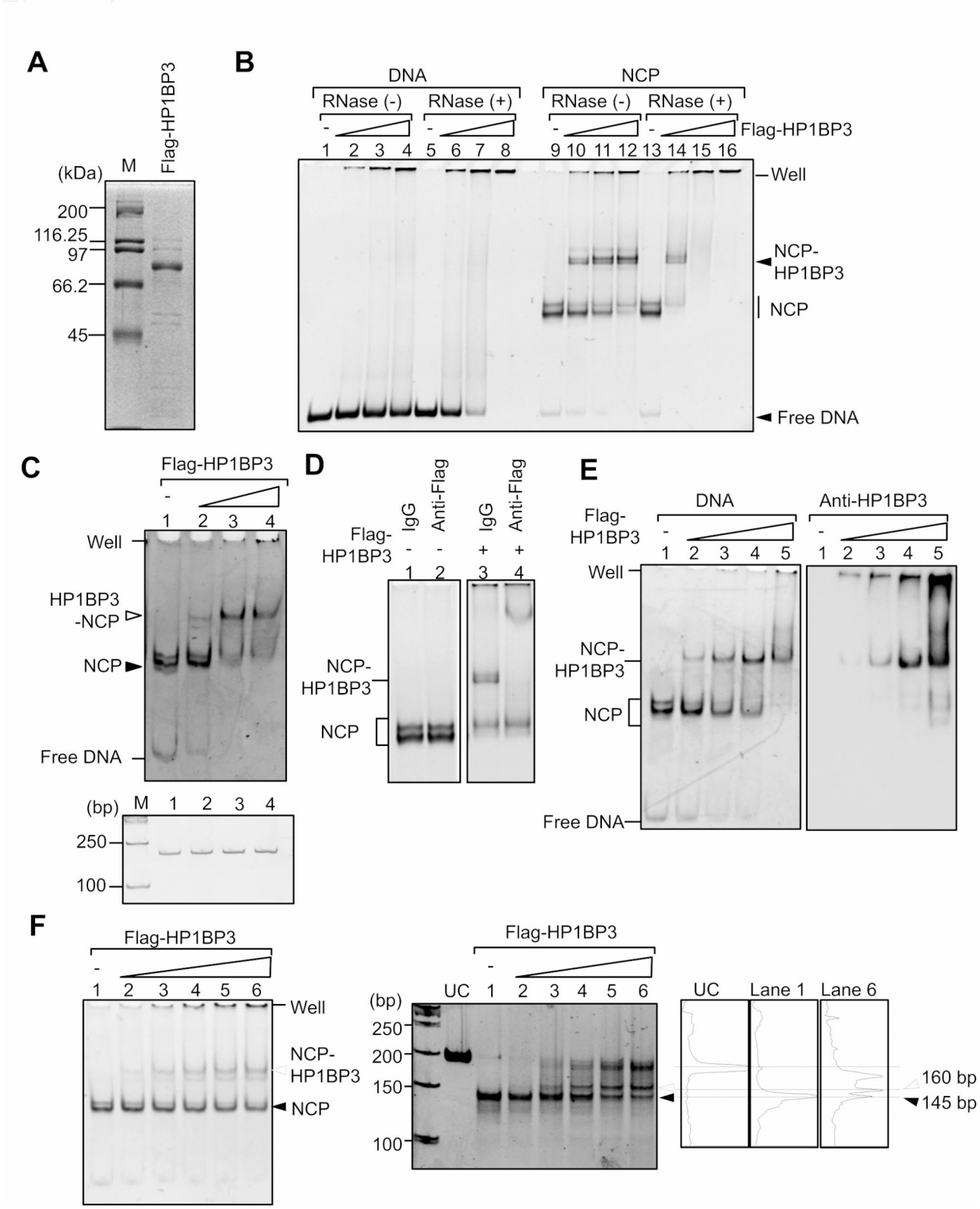

Fig. 2 (See legend on next page.)

(See figure on previous page.)

Fig. 2 HP1BP3 forms a chromatosome-like complex with NCPs. (**A**) Purified HP1BP3. Flag-tagged HP1BP3 was expressed in 293T cells and purified with Flag-M2 agarose beads. The protein was separated by 10% SDS-PAGE and visualized with CBB staining. Lane M indicates molecular weight markers. (**B**) DNA and NCP binding activity of HP1BP3. Flag-tagged HP1BP3 (0.2, 0.4, and 0.8 pmole) treated without (lanes 1–4 and 9–12) or with (lanes 5–8 and 13–16) RNase A as shown at the top of the lanes was incubated with 5 S rDNA (0.1 pmole) or NCP assembled on the same DNA. The complexes were loaded on 6% polyacrylamide gel in 0.5×TBE and DNA was visualized with Gel Red staining. Positions of DNA, NCPs, and the HP1BP3-NCP complex are shown at the right side of the panel. (**C**) DNA stability after incubation with HP1BP3. NCP (0.2 pmole) was incubated without or with increasing amounts of HP1BP3 as in B. The experiments were performed in duplicates and the one tube is loaded on native PAGE as in B (top panel), while the other tube was subjected to DNA extraction and separation by PAGE (bottom panel). Positions of free DNA, NCP, and NCP-HP1BP3 are indicated at the left side of the top panel. Lane M of the bottom panel indicates molecular weight markers. (**D**) HP1BP3 binding to NCPs. NCPs (0.2 pmole) were incubated without (lanes 1 and 2) or with (lanes 3 and 4) Flag-HP1BP3 (0.4 pmole) in the presence of mouse immunoglobulin (Ig, lanes 1 and 3) or anti-Flag antibody (lanes 2 and 4) (0.2 µg proteins for each antibody). The mixture was separated by 6% PAGE and DNA was visualized by Gel Red staining. (**E**) Western blotting of NCP-HP1BP3 complex. NCPs (0.2 pmole) was incubated without (lane 1) or with increasing amounts of HP1BP3 (0.1, 0.2, 0.4, and 0.8 pmole for lanes 2–5), separated on native PAGE, and DNA was visualized with GelRed staining (left panel). The gel was transferred to a PVDF membrane, followed by western blotting with anti-HP1BP3 antibody (right panel). Positions of Free-DNA, NCP, and NCP-HP1BP3 are shown at the left side of the panels. (**F**) MNase digestion of the NCP-HP1BP3 complex. NCPs (0.2 pmole) incubated without (buffer) or with Flag-HP1BP3 (0.05, 0.1, 0.2, 0.3 and 0.4 pmole) as in B were loaded on native PAGE (left panel). The same reaction was repeated and NCP samples were treated with micrococcus nuclease (MNase, 1 unit) at 37 °C for 1 min, followed by extraction of DNA (right panel). The band intensities of lanes UC (DNA untreated with MNase as a control), lanes 1 and 6 were scanned by the Image J software and plotted as shown at the right side of the panel. The size of the bands detected at peaks was estimated using molecular weight markers in lane M as a standard

purified (Fig. 2A). Although minor associated proteins were detected in the HP1BP3 sample, the Flag-HP1BP3 protein was purified as approximately 75 kDa protein. HP1BP3 demonstrated binding to a 196 bp-long 5 S rDNA, resulting in the detection of smear-shifted DNA on the gel (Fig. 2B, lanes 2–4). Furthermore, the HP1BP3 sample pre-treated with RNase A exhibited a greater capacity to bind the DNA than the sample without RNase A treatment (lanes 6–8). This suggests that the HP1BP3 sample contained RNA molecules that competitively inhibited the non-specific DNA binding activity of HP1BP3. To detect RNAs in the Flag-HP1BP3 sample, the protein solution preincubated without or with RNase A was separated by 6% PAGE (Supplementary Fig. 1). We found that nucleic acids stained by GelRed were detected at the well of the gel, which disappeared upon RNase A treatment. This indicated that some RNA molecules were co-purified with HP1BP3. In addition, excess HP1BP3 formed aggregates with DNA that did not enter the gel that was detected at the well of the gel. Because RNAs copurified with HP1BP3 disappeared upon RNase treatment (Supplementary Fig. 1), the nucleic acids detected at the well in Fig. 1B (lanes 6–8) should be 5 S rDNA fragment. Our results also demonstrated that both RNase A-treated and non-treated HP1BP3 bound to NCPs reconstituted with recombinant histones, resulting in the appearance of distinct shifted bands (lanes 10–12 and 14). The RNase A-treated HP1BP3 exhibited a markedly elevated binding affinity for NCP and DNA compared to the untreated HP1BP3. It is noteworthy that the co-purified RNAs were observed to inhibit the DNA binding activity of HP1BP3, but not efficiently the NCP binding activity (see Fig. 2B, lanes 2–4 and 10–12). This suggests that the co-purified RNAs may facilitate HP1BP3 binding to NCPs in a manner analogous to that of histone chaperones. Furthermore, the binding efficiency of HP1BP3 to nucleosomal DNA was significantly higher than that to linear, naked DNA, indicating a preference for the former over the latter. The amount of DNA at the well exhibited non-consistency with that of free DNA and NCP (see lanes 8 and 16). This raised the possibility that the DNA was degraded by the presence of excess HP1BP3. To exclude this possibility, DNA was extracted from the NCPs incubated without or with increasing amounts of HP1BP3 and separated by native PAGE (Fig. 2C). The results demonstrated that DNA was similarly recovered from the NCP samples incubated without or with increasing amounts of HP1BP3. The amount of DNA at the well of the gel appeared to be lower than that of the free DNA and NCP bands (lanes 1 and 9 in Fig. 2B). This was likely because the DNA at the well was partially removed during DNA staining.

To verify that the NCP bands that exhibited a shift in their migration upon the addition of HP1BP3 contained HP1BP3, a super-shift assay was conducted. The incubation of NCP with Flag-HP1BP3 resulted in NCP binding with Flag-HP1BP3, which migrated slower than NCP (Fig. 2D, lanes 1 and 3). The shifted band by Flag-HP1BP3 addition showed a super-shift by the presence of Flag antibody, while the super-shifted band by Flag antibody was not observed when NCP alone was incubated with anti-Flag antibody (Fig. 2D, lanes 2 and 4). To further confirm that the mobility of NCP was delayed by the presence of HP1BP3 and the shifted band contained HP1BP3, western blotting was performed after separation of the NCP-HP1BP3 complex by native PAGE (Fig. 2E). DNA in NCP was shifted by the presence of increasing amounts of HP1BP3 (lanes 2–5). The results of western blotting with anti-HP1BP3 revealed that the shifted band, but not NCP alone (lane 1), clearly contained HP1BP3 (Fig. 2E, right panel, lanes 2–5). These results indicated that HP1BP3 binds to NCPs and the bands shifted on native PAGE by the presence of HP1BP3 correspond to the NCP-HP1BP3 complex.

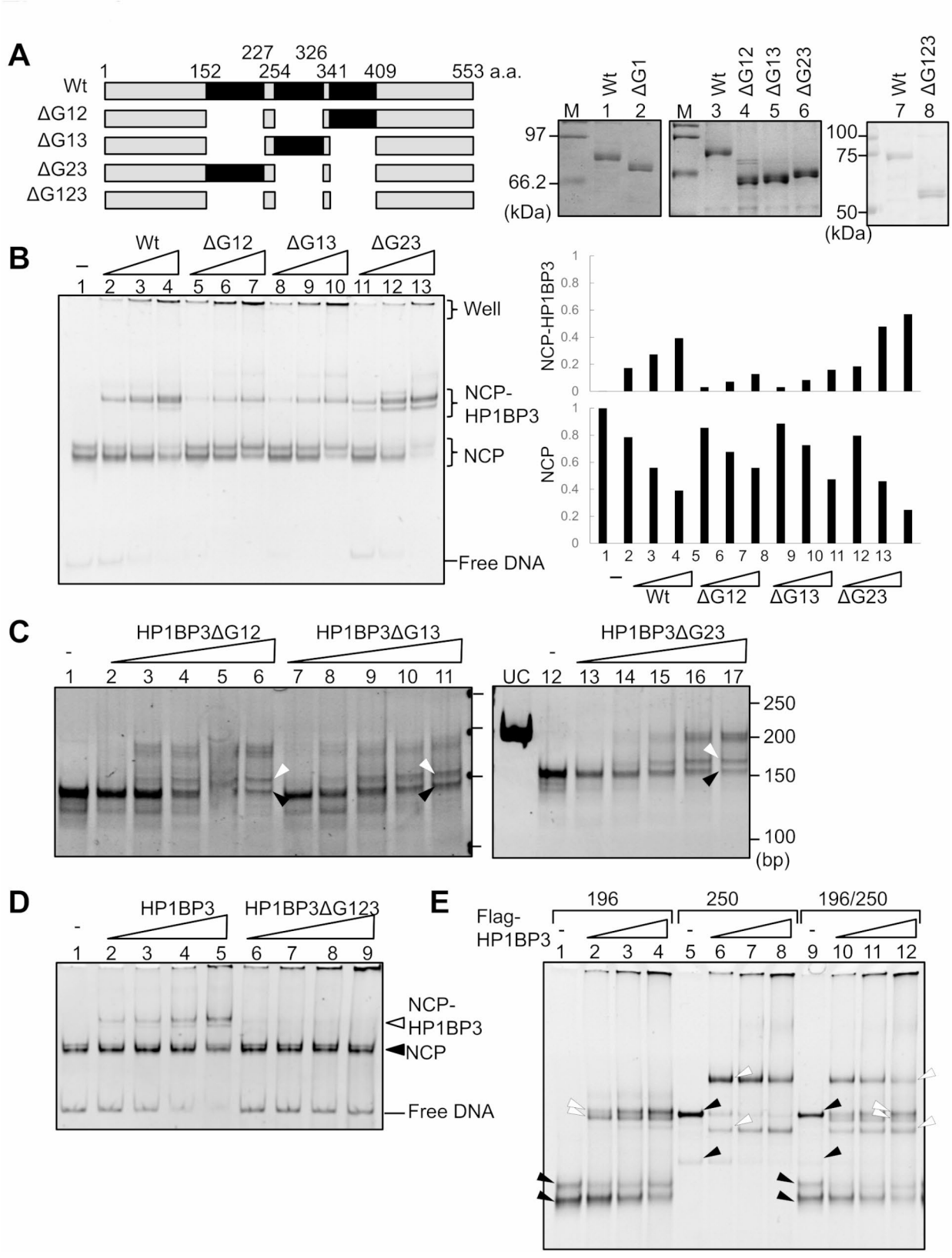

Fig. 3 (See legend on next page.)

(See figure on previous page.)

Fig. 3 Three globular domains of HP1BP3 bind redundantly to NCPs. (**A**) Preparation of the globular domain mutants of HP1BP3. HP1BP3 and its mutants lacking two of three globular domains, G1 (amino acids 152–227), G2 (amino acids 254–336), and G3 (amino acids 341–409), are represented schematically. ΔG12, ΔG13, and ΔG23 lack two globular domains as indicated. HP1BP3 mutant lacking all globular domains, ΔG123, was also prepared. The Flag-tagged HP1BP3 proteins were expressed in 293T cells and purified with Flag-M2 agarose beads. The proteins (500 ng) were separated by 10% SDS-PAGE and visualized by CBB staining. Lanes M indicate molecular weight markers. (**B**) NCP binding activity of HP1BP3 globular domain mutants. NCPs (0.1 pmole) were incubated with increasing amounts wild type HP1BP3 (lanes 2–4), HP1BP3ΔG12 (lanes 5–7), HP1BP3ΔG13 (lanes 8–10), and HP1BP3ΔG23 (lanes 11–13) (0.04, 0.1, and 0.2 pmole for each protein) and separated by 6% native PAGE in 0.5×TBE. DNA was visualized by Gel Red staining. The bands for NCPs and NCP-HP1BP3 complexes were quantitatively analyzed by Image J and the data are shown at the right side of the panel. (**C**) MNase digestion assay of NCP-HP1BP3 mutant complexes. NCPs (0.2 pmole) incubated without (buffer, lanes 1 and 12) or with Flag-HP1BP3 ΔG12, ΔG13, and ΔG23 (lanes 2–6, 7–11, and 13–17, respectively) (0.05, 0.1, 0.2, 0.3 and 0.4 pmole) were treated with micrococcus nuclease (MNase, 1 unit) at 37 °C for 1 min (right panel), followed by gel extraction and electrophoresis on PAGE. Positions of molecular weight markers are indicated at the right side of the panels. In lane UC, DNA was extracted without MNase digestion. (**D**) The globular domains of HP1BP3 are essential for its NCP binding. NCPs (0.1 pmole) was incubated without (lane 1) or with increasing amounts of HP1BP3 wild type and HP1BP3 ΔG123 (lanes 2–5 and 6–9, respectively) (0.1, 0.2, 0.3, and 0.4 pmole) and the complexes were separated by native PAGE. Positions of NCPs, NCP-HP1BP3, and free DNA are shown at the right side of the panel. (**E**) HP1BP3 recognizes single NCP. NCPs were assembled on 196 bp–5 S rDNA and 250 bp-Widom DNA. The 196 bp-NCPs (lanes 1–4) and 250 bp-NCP (lanes 5–8) (0.1 pmole each) were mixed with increasing amount of HP1BP3 (0.2, 0.4, and 0.8 pmole). In lanes 9–12, 196 bp-NCP and 250 bp-NCP (0.1 pmole each) were mixed with increasing amounts of HP1BP3 (0.2, 0.4, and 0.8 pmole). The complexes were incubated and separated by 6% PAGE. DNA was visualized by Gel Red staining. Positions of 196 bp-NCPs and 250 bp-NCP are indicated at the left side of lane 1 and right side of lane 5, respectively, with filled arrowheads. Positions of 196 bp-NCP-HP1BP3 and 250 bp-NCP-HP1BP3 complexes are indicated at the left side of lane 2 and right side of lane 7, respectively, with blank arrowheads

It is well-established that linker histone H1 binds to nucleosomes at the linker DNA entry-exit sites to form a chromatosome, which protects approximately 160 base pairs (bp) of DNA from micrococcal nuclease (MNase) digestion [31]. We proceeded to examine whether approximately 160 bp of DNA was protected by MNase digestion of the HP1BP3-NCP complex with the aim of elucidating the functions of HP1BP3 as a linker histone. NCPs preincubated without or with increasing amounts of Flag-HP1BP3 were directly loaded on native PAGE (Fig. 2F, left panel) or treated with MNase, after which DNA extraction and polyacrylamide gel electrophoresis were performed (Fig. 2F, middle panel). The image for lane UC (DNA non-treated with MNase), lane 1, and lane 6 were scanned and plotted as shown at the right panel of Fig. 2F. The data revealed that approximately 140–150 bp of DNA was protected when NCP alone was treated with MNase (lane 1), while the bands representing 160 bp DNA were increased when increasing amounts of Flag-HP1BP3 was added (lanes 3–6, and scanned plot for lanes 1 and 6). The bands between 180 and 200 bp were also increased by the addition of increasing amounts of HP1BP3. The increase in the DNAs with 180 to 200 bp suggests that HP1BP3 could randomly bind to linker DNA extended from NCPs, which inhibits MNase access.

The central region of HP1BP3 is comprised of three linker histone-like globular domains (see Fig. 1). We wondered how these three domains cooperatively or independently bind to NCP. To address this question, three mutant proteins lacking two of the three globular domains were prepared and designated ΔG12, ΔG13, and ΔG23 (Fig. 3A). We also prepared the mutant HP1BP3 protein lacking all three globular domains ΔG123. It was observed that the mutant proteins ΔG12, ΔG13, and ΔG23 exhibited a similar binding capacity to NCPs as the wild type full-length HP1BP3 (Fig. 3B), with a slight difference in binding efficiency. To quantitatively analyze the data, the band intensity of NCPs and NCP-HP1BP3 complex was measured (Fig. 3B, right panel). The NCP bands decreased, while the NCP-HP1BP3 complex increased by the addition of increasing amounts of HP1BP3. The increase in the NCP-HP1BP3 complex was lower for ΔG13 and ΔG12 than for HP1BP3 full-length and ΔG23. These results suggest that the affinity for NCPs of G1 is higher than those of G2 and G3.

Although the binding affinity to NCP may be different for each globular domain, the HP1BP3 mutants ΔG12, ΔG13, and ΔG23, which have one of the three globular domains, induced similar band shift of NCPs on native PAGE (Fig. 3B). We wondered whether these mutants bind NCPs like the globular domain of linker histone H1. To address this point, we performed MNase digestion assay (Fig. 3C). When NCP alone was subjected to MNase digestion, the DNA between 140 and 150 bp was protected from MNase digestion (lanes 1 and 12), which is consistent with the data shown in Fig. 2F. When NCP was preincubated with increasing amounts of HP1BP3 mutants, ΔG12, ΔG23, and ΔG13, the bands with around 160 bp appeared (shown by blank arrowheads in Fig. 3C). Thus, it is strongly suggested that the three globular domains of HP1BP3 have the potential ability to independently and redundantly bind NCPs.

To verify that the globular domains of HP1BP3 are responsible for NCP binding, a mutant protein lacking all GDs (HP1BP3ΔG123) were prepared and NCP binding activity was examined (Fig. 3D). NCPs were incubated with increasing amounts of full-length HP1BP3 or ΔG123, followed by separation on native PAGE. HP1BP3 bound NCPs and shifted bands were observed. On the other hand, the shifted band was not observed even in the presence of excess ΔG123. Since nucleic acids was increased at the well of the gel upon the addition of

increasing amounts of ΔG123, this protein was also possible to contain RNAs. These results support our conclusion that the globular domains of HP1BP3 are responsible for NCP binding.

Given that three globular domains of HP1BP3 are capable of independently binding NCPs, it was postulated that a single molecule of HP1BP3 could potentially interact with three NCPs. If this is indeed the case, it would suggest that HP1BP3 may contribute to the formation of high-order chromatin structures via different mechanisms to those observed in linker histone H1s. To investigate this hypothesis, NCPs were prepared with either 196 bp-DNA or 250 bp-DNA, and binding assays were conducted (Fig. 2E). The binding of HP1BP3 to the 196 bp-NCP and 250 bp-NCP was observed to be of a similar efficiency, resulting in the appearance of shifted bands (lanes 2–4 and 6–8, blank arrowheads). Upon incubation of HP1BP3 with both 196 bp-NCP and 250 bp-NCP in a tube, only the bands corresponding to 196 bp-NCP-HP1BP3 or 250 bp-NCP-HP1BP3 were observed (lanes 10–12). These results strongly suggest that HP1BP3 is capable of recognizing a single NCP, but unable to link two or three NCPs together. It appeared that only one globular domain of the three globular domains of HP1BP3 is capable of recognizing NCPs.

Because DNA and NCP binding properties of HP1BP3 were analogous to those of linker histone H1s and that the latter was regulated by linker histone chaperones. We previously demonstrated that NPM1 and TAF-Iβ bind to linker histones, thereby regulating their DNA/NCP binding activity [16, 17]. Therefore, it was ascertained whether these linker histone chaperones were capable of binding to HP1BP3. Nuclear extracts from HeLa cells were prepared, and an immunoprecipitation assay was conducted using a specific antibody against HP1BP3 (Fig. 4A). The results demonstrated that endogenous HP1BP3 co-precipitated with NCL, NPM1, and TAF-Iβ. However, co-immunoprecipitation of HP1BP3 with an abundant replication factor, proliferating cell nuclear antigen (PCNA), was not observed (lane 6). To confirm the direct binding between histone chaperones and HP1BP3, GST-pull down assays were conducted (Fig. 4B). GST, GST-NPM1, and GST-TAF-Iβ were incubated in the absence or presence of HP1BP3, and the bound proteins were analyzed by SDS-PAGE. The results demonstrated that GST-NPM1 and GST-TAF-Iβ, but not GST, co-precipitated with Flag-HP1BP3 (lanes 6 and 7). To determine the region(s) of HP1BP3 responsible for interacting with histone chaperones, three mutant proteins, HP1BP3-N, -M, and -C were prepared and GST-pull down assays were conducted (Fig. 4C). The results demonstrated that GST-NPM1 and GST-TAF-Iβ efficiently co-precipitated HP1BP3-M (lanes 11 and 12) and HP1BP3-C (lanes 14 and 15). Based on these findings, it can be concluded that HP1BP3 binds to linker histone chaperones through its central globular domains and the C-terminal disordered region.

We next examined the effects of histone chaperones on the NCP binding activity of HP1BP3. To this end, GST-NPM1 and GST-TAF-Iβ were purified (Fig. 5A). NCPs assembled on 196-bp DNA were incubated with higher concentration of HP1BP3 preincubated without or with increasing amounts of histone chaperones or GST, and the complexes were analyzed by native PAGE (Fig. 5B). When an excess amount of HP1BP3 alone was incubated with NCPs, the complexes did not enter the gel, and a minor population of the DNA was detected (lane 2). Preincubation of HP1BP3 with GST alone did not affect the NCP binding of HP1BP3 (lane 15). Under this condition, when an excess amount of HP1BP3 was preincubated with increasing amounts of GST-NPM1 or GST-TAF-Iβ, HP1BP3-NCPs complexes were properly formed (indicated by a filled arrowhead). By incubating with GST-NPM1 or GST-TAF-Iβ, not only HP1BP3-NCP complexes but the bands corresponding to free NCPs were also increased. Furthermore, when the amounts of GST-TAF-Iβ was increased, only NCPs, but not HP1BP3-NCP, were formed (lanes 12–14). These results indicated that both NPM1 and TAF-Iβ similarly suppress the excess binding of HP1BP3 to NCPs, and TAF-Iβ shows the ability to inhibit the formation of HP1BP3-NCPs or remove HP1BP3 from the HP1BP3-NCP complexes.

We subsequently analyzed the impacts of these linker histone chaperones on the HP1BP3 functions within cells. EGFP-tagged HP1BP3 was transiently expressed in U2OS cells, and fluorescence recovery after photobleaching (FRAP) assays were conducted. EGFP-HP1BP3 was clearly detected in the nucleus, and this pattern was not affected by NPM1 or TAF-Iβ siRNA treatment (Fig. 5C and Supplementary Fig. 2). The expression level of TAF-Iβ was efficiently depleted by siRNA (Fig. 5D), whereas that of NPM1 was reduced to approximately 30% of the control cells. It was also demonstrated that the expression level of HP1BP3 normalized to that of β-actin remained relatively unchanged following TAF-I and NPM1 siRNA treatments (see quantitative data shown at the bottom of Fig. 5Dl). The EGFP signals were bleached by a 488-nm laser line, and the EGFP intensity was measured at one-second intervals over a two-minute period (Fig. 5E). In cells treated with control siRNA, the EGFP signal was recovered to 80% of its initial intensity, indicating that HP1BP3 may undergo dynamic association with or dissociation from chromatin. The dynamic behavior of HP1BP3 was found to be similar to those observed for linker histone H1s [32]. NPM1 siRNA treatment did not result in any change in the localization and dynamics of HP1BP3. However, when TAF-Iβ was depleted, a significant decrease in the dynamics of HP1BP3 mobility

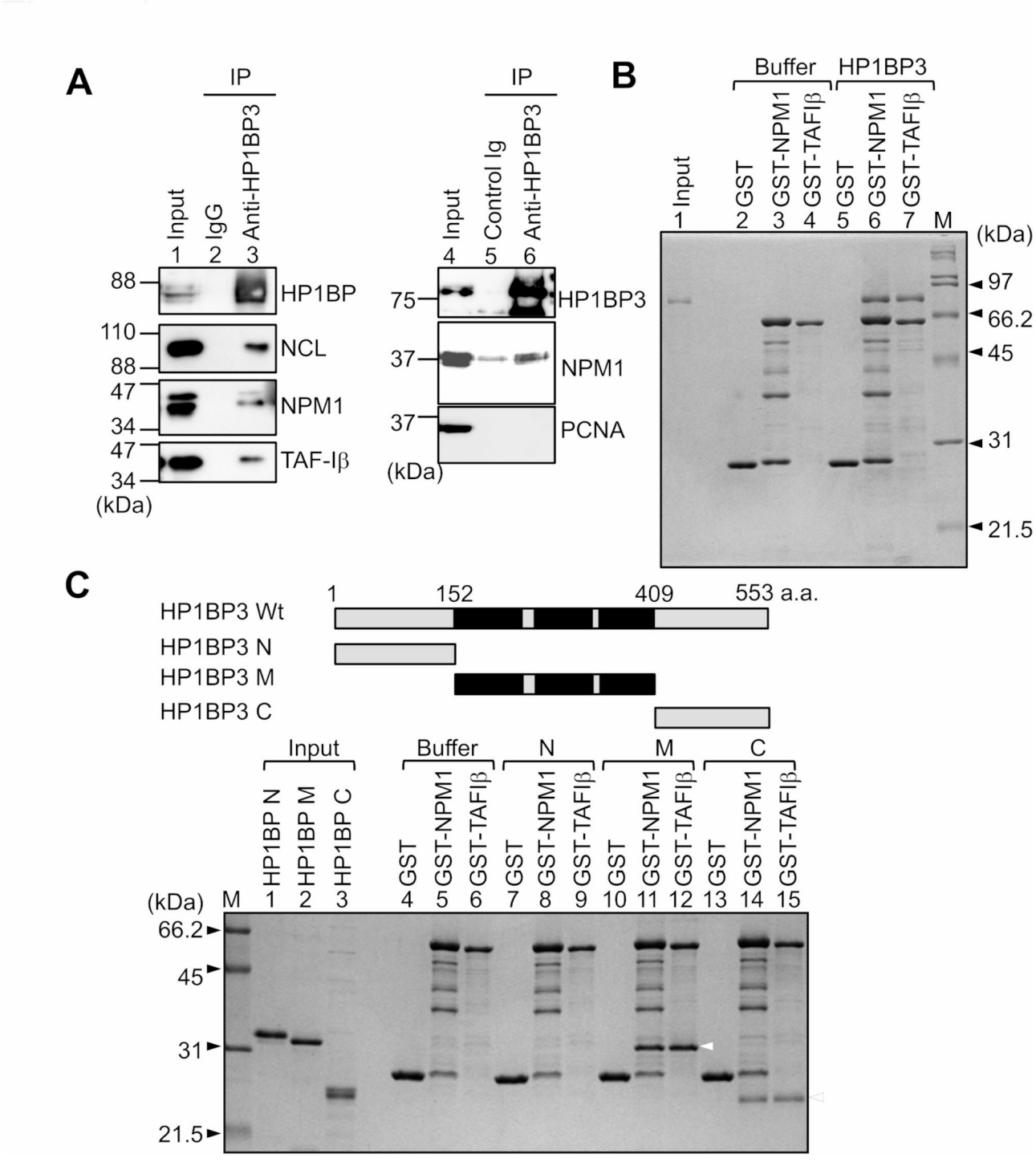

Fig. 4 HP1BP3 binds to linker histone chaperones, NPM1 and TAF-I. (**A**) Immunoprecipitation of HP1BP3. HeLa cell nuclear extracts were mixed with control rabbit Ig or anti-HP1BP3 antibody (2 μg each) and incubated at 4 °C for 2 h. Protein A sepharose beads were added and incubated for an additional 30 min. The beads were washed extensively, and the proteins bound to the beads were eluted by an SDS-PAGE sample buffer, followed by 10% SDS-PAGE and western blotting with anti-HP1BP3, NCL, NPM1, and TAF-Iβ (lanes 2 and 3). The same experiment was repeated and western blotting with anti-HP1BP3, NPM1, and PCNA antibodies were performed (lanes 5 and 6). Input extracts (1%) were loaded in lanes 1 and 4. (**B**) GST-pull down assay. GST, GST-NPM1, and GST-TAF-Iβ (1 μg each) immobilized on glutathione Sepharose beads, mixed with buffer alone (lanes 2–4) or 1 μg of Flag-HP1BP3 (lanes 5–7) and incubated for 2 h. The beads were washed extensively, and the proteins bound to the beads were eluted and analyzed by 10% SDS-PAGE. The proteins were visualized by CBB staining. In lane 1, input Flag-HP1BP3 (100 ng) was loaded. Lane M is a molecular weight marker. (**C**) The NPM1- and TAF-I-binding domain of HP1BP3. GST, GST-NPM1, and GST-TAF-Iβ were immobilized and HP1BP3 mutants, HP1BP3-N, HP1BP3-M, and HP1BP3-C were added and incubated for 2 h. The bound proteins were analyzed as in **B**. The blank arrowheads shown at the right side of lanes 12 and 15 indicate the positions of HP1BP3-M and HP1BP3-C

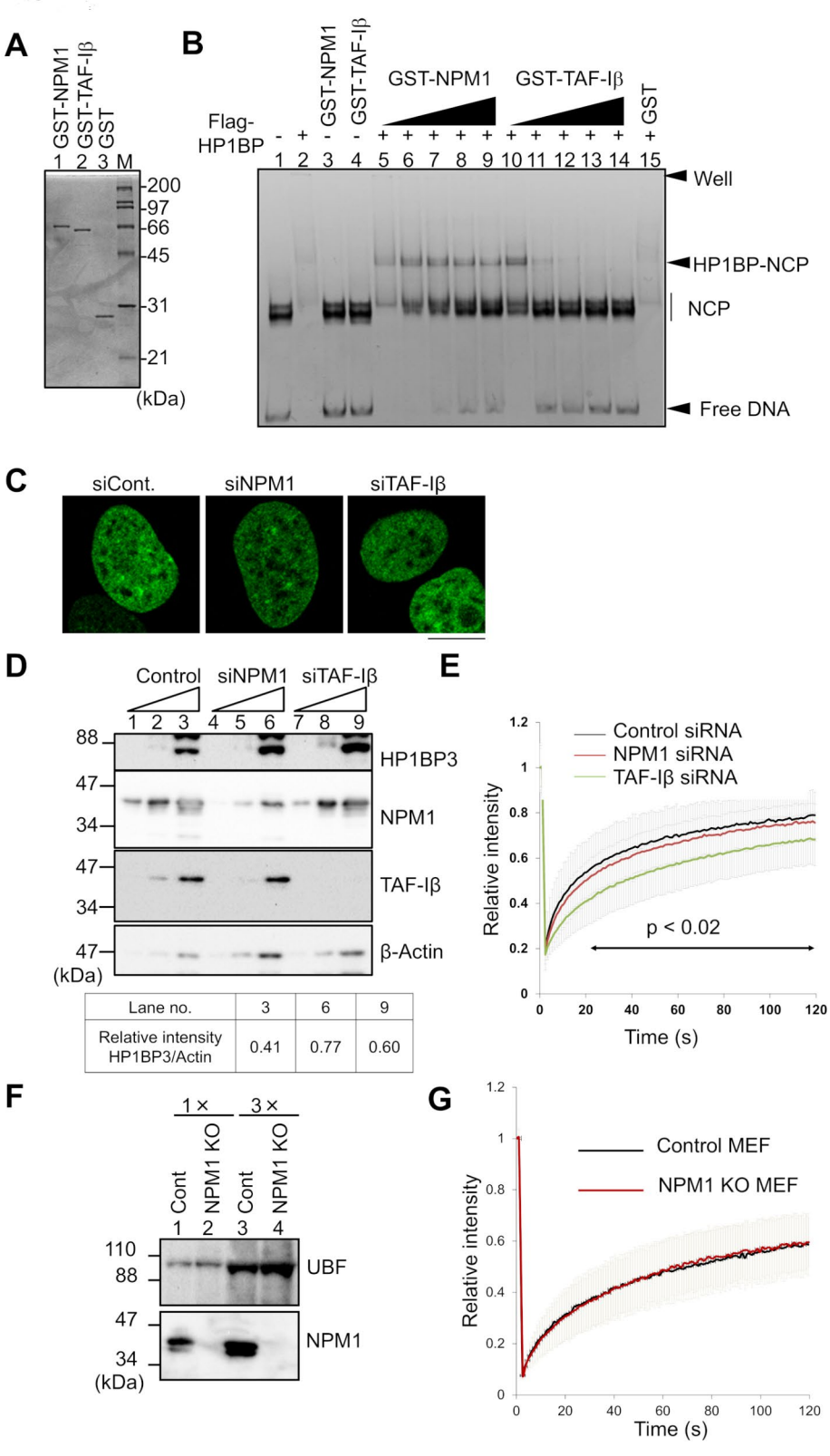

Fig. 5 (See legend on next page.)

(See figure on previous page.)

Fig. 5 Effects of NPM1 and TAF-I on the chromatin binding activity of HP1BP3. (**A**) Purified GST-NPM1, GST-TAF-Iβ, and GST. The GST proteins (200 ng) were separated by 10% SDS-PAGE and visualized by CBB staining. The positions of molecular weight markers are shown at the right side of the panel. (**B**) NPM1 and TAF-Iβ inhibit the nonspecific binding of HP1BP3 to NCPs. 5S rDNA NCP (0.1 pmole) was incubated without (lane 1, 3, and 4) or with (lanes 2 and 5–14) Flag-HP1BP3 (0.8 pmole). In lanes 5–9 and 10–14, GST-NPM1 and GST-TAF-Iβ (0.4, 0.8, 1.6, 3.2, and 4.8 pmole) were also added. In lane 15, GST (4.8 pmole) was added as a control. The mixture was incubated at 30 °C for 30 min and loaded on 6% PAGE. Positions of free DNA, NCP, and the HP1BP3-NCP complex are shown at the right side of the panel. (**C**) Localization of HP1BP3 in U2OS cells treated with siRNAs. U2OS cells were transfected with control siRNA, NPM1 siRNA, and TAF-Iβ siRNA as indicated and the plasmid for the expression of EGFP-HP1BP3 was transfected 48 h after siRNA transfection. The localization of EGFP-HP1BP3 were observed 72–80 h post plasmid transfection under a confocal microscope. A bar shown at the right bottom indicates 10 μm. (**D**) Expression of NPM1 and TAF-Iβ in siRNA treated cells. U2OS cells treated with siRNAs as in C were subjected to western blotting with antibodies against HP1BP3, NPM1, TAF-Iβ, and actin. Proteins from 1×10^4, 3×10^4, and 1×10^5 cells were loaded for each sample. The band intensity of HP1BP3 and β-actin in lanes 3, 6, and 9 was analyzed by Image J and the ratio HP1BP3/β-actin for lanes 3, 6, and 9 are shown at the bottom of the panel. (**E**) FRAP analyses of EGFP-HP1BP3. U2OS cells transfected with siRNA and EGFP-HP1BP3 plasmid as in C were grown in glass-based dishes and subjected to FRAP analyses. The EGFP signals were bleached with a 488-nm lase line and the recovery of the EGFP signals was measured with one-second interval for two-minutes and plotted as a function of time (s). For each sample, 10 cells were examined and the data shown were averaged. The error bars indicate ± SD. The recovery rates of HP1BP3 in NPM1- and TAF-I-knockdown cells were statistically analyzed by student t-test and the data for TAF-I knockdown cells (from 14 to 120 s after photo bleach) relative to those of control cells were $p < 0.02$. (**F**) Expression of NPM1 in NPM1 KO MEF cells. Proteins from control MEF cells and NPM1 knockout MEF cells (3×10^4 and 1×10^5 cells for lanes 1 and 2, and 3 and 4) were separated by SDS-PAGE and subjected to western blotting with anti-UBF and anti-NPM1 antibodies. (**G**) FRAP assay with NPM1 KO cells. EGFP-HP1BP3 was transiently expressed in control (black) and NPM1 KO (red) MEF cells and FRAP assay as in E were conducted

was observed. This result indicated that TAF-Iβ plays an important role in the maintenance of the chromatin association-dissociation cycle of HP1BP3. To more accurately evaluate the effect of NPM1 on the dynamic behavior of HP1BP3, we took advantage of NPM1 knockout (KO) mouse embryonic fibroblast (MEF) cells. The expression of NPM1 was not detected in NPM1 KO MEF cells, whereas a rRNA transcription factor, UBF, was similarly expressed both in control and NPM1 KO MEF cells (Fig. 5F). EGFP-HP1BP3 was transiently expressed in both control and NPM1 KO MEF cells and FRAP assay was conducted (Fig. 5G). The results revealed that the recovery rate of the EGFP signal was not influenced by NPM1 KO, indicating that NPM1 is dispensable for the dynamics of HP1BP3.

Finally, we conducted ChIP-Seq analyses to examine the localization patterns of HP1BP3 throughout the genome. For comparison, ChIP-Seq analysis with linker histone H1.2 was also conducted. Furthermore, to investigate the influence of histone chaperones, NPM1 and TAF-Iβ on the chromatin binding of HP1BP3 and H1.2, cells treated with NPM1 siRNA or TAF-Iβ siRNA were subjected to ChIP-Seq analyses (Fig. 6). HeLa cells transfected with control siRNA, NPM1 siRNA, or TAF-Iβ siRNA were fixed with 0.5% formaldehyde and ChIP was conducted with anti-HP1BP3 and anti-H1.2 specific antibodies. The precipitated DNA was subjected to deep sequence analyses. The data demonstrated that HP1BP3 and H1.2 distributed throughout the genome with weak distinct preferences. Representative genomic loci bound by HP1BP3 and H1.2 were illustrated in Fig. 6A. We observed that H1.2 was more abundant than HP1BP3 at some loci (e.g., that on chromosome 8), whereas HP1BP3 exhibited a greater enrichment than H1.2 at other loci (e.g., that on chromosome 19). This was evident when the distinct distributions of HP1BP3 and H1.2 were examined as log2 fold change (log2fc) between them. Furthermore, when the enrichment of histone active (H3K4me3 and H3K27ac) and inactive marks (H3K9me3 and H3K27me3) was compared to those of HP1BP3 and H1.2, HP1BP3 exhibited a preference for binding to regions with high levels of active histone marks, whereas H1.2 demonstrated a preference for binding to regions with high levels of inactive histone marks. This pattern was also observed when the top-1000 genomic regions enriched for HP1BP3 and H1.2 binding were compared to the distribution patterns of active and inactive histone marks (Fig. 6B).

The overall distribution patterns of HP1BP3 and H1.2 remained largely unaltered upon NPM1 or TAF-Iβ knockdown, as illustrated in Fig. 6A. However, we observed that at the loci where HP1BP3 was more abundantly enriched, HP1BP3 binding exhibited a tendency to reduce, whereas H1.2 binding demonstrated a tendency to increase upon NPM1 and TAF-Iβ knockdown (Fig. 6A, bottom panel and Fig. 6B, top panels). Conversely, at the loci where H1.2 was more abundant, H1.2 binding exhibited a tendency to reduce, whereas HP1BP3 binding demonstrated a tendency to increase by NPM1 and TAF-Iβ knockdown. Indeed, the genome-wide correlation coefficients indicated that changes in H1.2 and HP1BP3 binding upon chaperone knockdown were positively and inversely correlated, respectively, with the HP1BP3 vs. H1.2 distribution (Fig. 6C). These results suggest that NPM1 and TAF-Iβ play redundant roles in determining the preferential binding loci of HP1BP3 and H1.2.

Discussion

While we are unable to conclude that HP1BP3 binds NCP at a ratio of 1:1 as do canonical linker histones, our findings imply that HP1BP3 is a non-typical linker histone that possesses three globular domains in its central regions. Our findings demonstrated that HP1BP3 efficiently binds to NCPs (Fig. 2). Furthermore, MNase

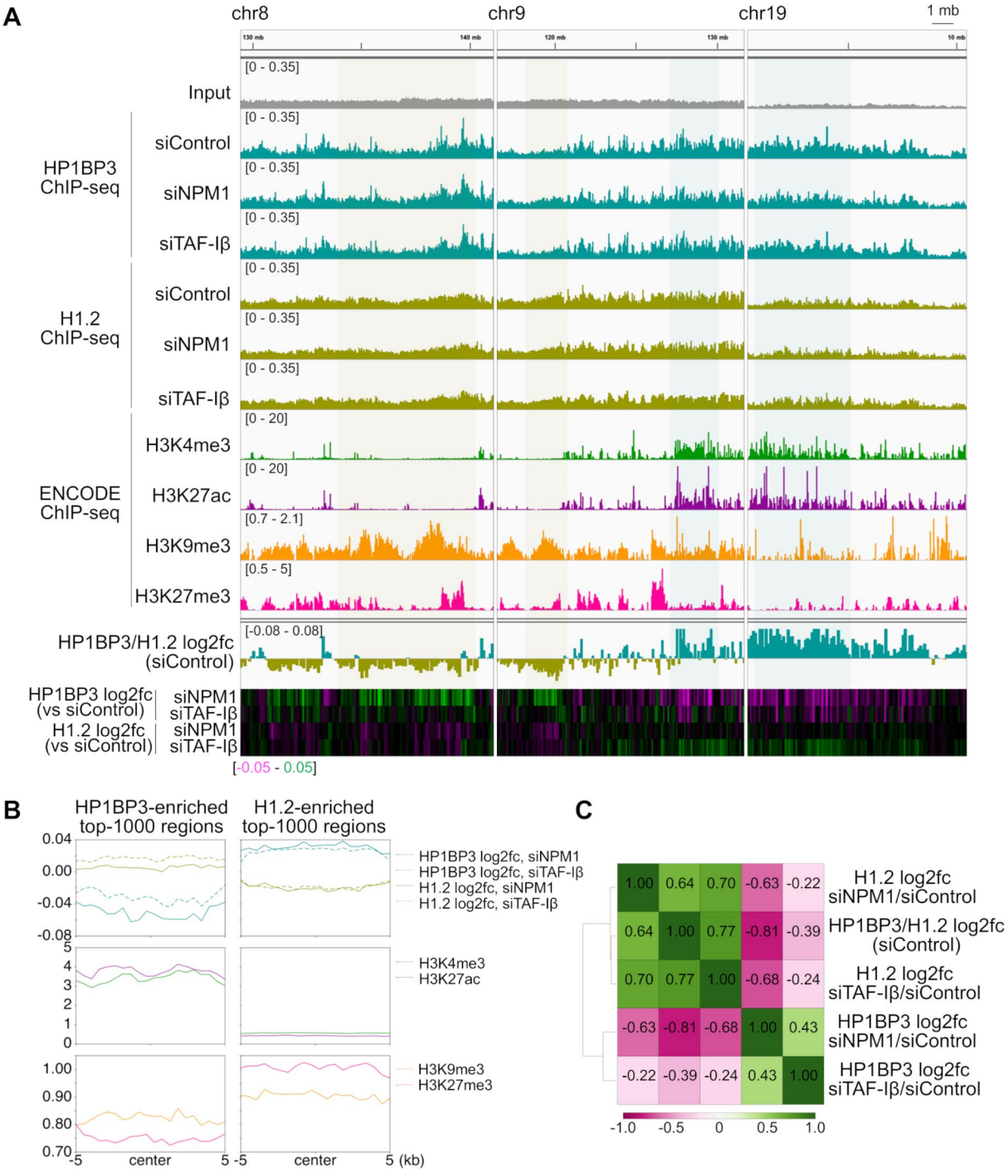

Fig. 6 Distribution of HP1BP3 and H1.2 throughout the genome and the effects of linker histone chaperones on their chromatin binding. (**A**) Representative screenshots of ChIP-Seq tracks. HeLa cells treated with control siRNA, NPM1 siRNA, TAF-Iβ siRNA were fixed with 0.5% formaldehyde and chromatin immunoprecipitation was conducted with anti-HP1BP3 or anti-H1.2 antibodies. The precipitated DNA was subjected to deep sequencing. ChIP-Seq data for HP1BP3, histone H1.2, and the histone modifications were visualized on a genome browser. HP1BP3-enriched and H1.2-enriched genomic regions are highlighted with greenish and yellowish transparent boxes, respectively. Note that the bin size for the log2fc data is 100-kb. (**B**) Average levels of ChIP-Seq data at top-1000 genomic regions for HP1BP3 and H1.2 enrichment. Top-1000 genomic regions (10-kb window) for HP1BP3 and H1.2 enrichment were identified based on the log2fc values for HP1BP3/H1.2 binding in siControl cells. Aggregation plots for the top-1000 regions were generated with the indicated ChIP-Seq data. (**C**) Correlation between the log2fc ChIP-Seq data. A matrix based on Spearman correlation calculated in 1-mb bins across the entire genome is shown for the indicated datasets

digestion of the NCP-HP1BP3 complex produced 160 base pairs of DNA, which is similar in size to the protected DNA from MNase digestion of the NCP-H1 complex. The globular domains are capable of fitting and binding to the nucleosome entry/exit sites, and our data demonstrated that either one globular domain is sufficient for HP1BP3 to bind to NCP. From this observation, it was reasonable to speculate that a single HP1BP3 molecule could bind to three NCPs to form condensed chromatin structures. Contrary to this speculation, we found that a single HP1BP3 molecule recognizes only one NCP under our experimental conditions (Fig. 3E). It is conceivable that upon the binding of a globular domain to NCP, the remaining two globular domains may be rendered inaccessible to NCP. Given that the mutant HP1BP3 proteins lacking two of the three globular domains bind to NCPs with slightly different binding affinities, it can be inferred that all the globular domains have the potential to bind to NCPs. It is currently not understood how one globular domain among three is selected when HP1BP3 binds to NCPs. Furthermore, we cannot exclude the possibility that a single HP1BP3 molecule may recognize two or three NCPs when they are in a nucleosome array.

The genome-wide distribution patterns of linker histone variants have been investigated in breast cancer cell lines and mouse embryonic stem (ES) cells [7, 9]. The results demonstrate that each linker histone variant exhibits a preference for binding loci. For example, H1.2 is less abundant at the transcription start sites of inactive genes than other variants, whereas it is enriched at loci with low-guanine-cytosine content. Similarly, we observed that HP1BP3 and H1.2 exhibit weak, but distinct preferences for binding loci (Fig. 6). Therefore, it can be concluded that HP1BP3 and linker histone variants play redundant roles in regulating the chromatin structure, although they also play specific roles at their preferential binding sites.

The chromatin binding of HP1BP3 is regulated by linker histone chaperones, NPM1 and TAF-Iβ. Both NPM1 and TAF-Iβ exhibit comparable binding to the central globular domains and C-terminal region of HP1BP3 (Fig. 4). However, the association with and dissociation from chromatin of HP1BP3 within cells were regulated by TAF-Iβ, but not by NPM1 (Fig. 5). This may be because that the binding affinity of HP1BP3 to TAF-Iβ was higher than that observed to NCPs. However, we observed by ChIP-Seq analyses that the binding site preferences of HP1BP3 and H1.2 were obscured upon knockdown of both NPM1 and TAF-Iβ. These findings suggest an interesting possibility that the recruitment of linker histone variants, including HP1BP3, to their preferred genomic loci may require the involvement of the linker histone chaperone proteins, including NPM1 and TAF-Iβ. The linker histone chaperones may facilitate the transfer of linker histones to their preferred genomic loci through as-yet-unknown mechanisms, or they may impede the binding of linker histones to their non-preferred genomic loci.

Conclusions

Despite the suggestion that HP1BP3 functions as a linker histone, the full-length HP1BP3 protein has never been analyzed as a linker histone. In this manuscript, our data revealed that HP1BP3 binds NCPs in a manner similar to linker histone H1. Furthermore, the linker histone function of HP1BP3 was found to be regulated by the linker histone chaperones, NPM1 and TAF-Iβ. ChIP-Seq analyses revealed that HP1BP3 and H1.2 exhibit a weak but distinct binding site preference along the genome. An interesting finding is that the binding site preferences of HP1BP3 and H1.2 may be regulated by linker histone chaperones. Our results contribute to the understanding of the mechanisms by which linker histone variants regulate higher order chromatin structures.

Abbreviations

ChIP-Seq	Chromatin immunoprecipitation-sequence
FRAP	Fluorescence recovery after photobleaching
HP1BP3	Heterochromatin protein 1 binding protein 3
NCP	Nucleosome core particle
NPM1	Nucleophosmin
TAF-I	Template activating factor-I

Supplementary Information

The online version contains supplementary material available at https://doi.org/10.1186/s13072-025-00581-x.

Supplementary Material 1

Acknowledgements

We would like to thank Dr. Emanuela Colombo (European Institute of Oncology, Italy) for her generous gifts of p53-/- and p53-/-NPM1-/- MEFs and Mr. Yuichi Sakamoto (Kitasato University) for his help to analyze the ChIP-Seq data.

Author contributions

M.H., J.L. and M.O. conceived the project and designed the study. M.H., T.K., T.H., J.L., Y.O., and M.O. performed experiments and data analysis. T.K. and M.O. did bioinformatic data analysis. M.H., J.L., T.K., and M.O. analyzed the data and interpreted the outcomes. All authors participated in reviewing and interpretation of the data and writing the manuscript. All authors read and approved the final manuscript.

Funding

This work was supported by the joint research program of the Institute for Molecular and Cellular Regulation, Gunma University (Number 22010) to MO, JSPS KAKENHI (Grant Numbers 17K07300 and 26440021 to MO, Grant Numbers 23K07983 and 24H01222 to TK, and Takeda Science Foundation and Gunma Foundation for Medicine and Health Science to TK. This work was also supported in part by the MEXT Cooperative Research Project Program, Medical Research Center Initiative for High Depth Omics, and CURE: JPMXP1323015486 for MIB, Kyushu University (to YO).

Data availability

The ChIP-Seq data that support the findings of this study have been deposited in Gene Expression Omnibus with the accession number GSE275436.

Declarations

Competing interests
The authors declare no competing interests.

Received: 25 September 2024 / Accepted: 15 March 2025
Published online: 27 March 2025

References

1. Zhou BR, Feng H, Kale S, Fox T, Khant H, de Val N, Ghirlando R, Panchenko AR, Bai Y. Distinct structures and dynamics of chromatosomes with different human linker histone isoforms. Mol Cell. 2021;81(1):166–e182166.
2. Song F, Chen P, Sun D, Wang M, Dong L, Liang D, Xu RM, Zhu P, Li G. Cryo-EM study of the chromatin fiber reveals a double helix twisted by tetranucleosomal units. Science. 2014;344(6182):376–80.
3. Zhou BR, Feng H, Kato H, Dai L, Yang Y, Zhou Y, Bai Y. Structural insights into the histone H1-nucleosome complex. Proc Natl Acad Sci U S A. 2013;110(48):19390–5.
4. Fan Y, Nikitina T, Morin-Kensicki EM, Zhao J, Magnuson TR, Woodcock CL, Skoultchi AI. H1 linker histones are essential for mouse development and affect nucleosome spacing in vivo. Mol Cell Biol. 2003;23(13):4559–72.
5. Fan Y, Sirotkin A, Russell RG, Ayala J, Skoultchi AI. Individual somatic H1 subtypes are dispensable for mouse development even in mice lacking the H1(0) replacement subtype. Mol Cell Biol. 2001;21(23):7933–43.
6. Prendergast L, Reinberg D. The missing link. Genes Dev. 2021;35(1–2):40–58.
7. Cao K, Lailler N, Zhang Y, Kumar A, Uppal K, Liu Z, Lee EK, Wu H, Medrzycki M, Pan C, et al. High-resolution mapping of h1 linker histone variants in embryonic stem cells. PLoS Genet. 2013;9(4):e1003417.
8. Izzo A, Kamieniarz-Gdula K, Ramírez F, Noureen N, Kind J, Manke T, van Steensel B, Schneider R. The genomic landscape of the somatic linker histone subtypes H1.1 to H1.5 in human cells. Cell Rep. 2013;3(6):2142–54.
9. Millán-Ariño L, Islam AB, Izquierdo-Bouldstridge A, Mayor R, Terme JM, Luque N, Sancho M, López-Bigas N, Jordan A. Mapping of six somatic linker histone H1 variants in human breast cancer cells uncovers specific features of H1.2. Nucleic Acids Res. 2014;42(7):4474–93.
10. Li JY, Patterson M, Mikkola HK, Lowry WE, Kurdistani SK. Dynamic distribution of linker histone H1.5 in cellular differentiation. PLoS Genet. 2012;8(8):e1002879.
11. Le Douarin B, Nielsen AL, Garnier JM, Ichinose H, Jeanmougin F, Losson R, Chambon P. A possible involvement of TIF1 alpha and TIF1 beta in the epigenetic control of transcription by nuclear receptors. EMBO J. 1996;15(23):6701–15.
12. Andrews AJ, Chen X, Zevin A, Stargell LA, Luger K. The histone chaperone Nap1 promotes nucleosome assembly by eliminating nonnucleosomal histone DNA interactions. Mol Cell. 2010;37(6):834–42.
13. Wilhelm FX, Wilhelm ML, Erard M, Duane MP. Reconstitution of chromatin: assembly of the nucleosome. Nucleic Acids Res. 1978;5(2):505–21.
14. Nelson T, Wiegand R, Brutlag D. Ribonucleic acid and other polyanions facilitate chromatin assembly in vitro. Biochemistry. 1981;20(9):2594–601.
15. Okuwaki M, Matsumoto K, Tsujimoto M, Nagata K. Function of nucleophosmin/B23, a nucleolar acidic protein, as a histone chaperone. FEBS Lett. 2001;506(3):272–6.
16. Kato K, Okuwaki M, Nagata K. Role of template activating Factor-I as a chaperone in linker histone dynamics. J Cell Sci. 2011;124(Pt 19):3254–65.
17. Okuwaki M, Abe M, Hisaoka M, Nagata K. Regulation of cellular dynamics and chromosomal binding site preference of linker histones H1.0 and H1.X. Mol Cell Biol. 2016;36(21):2681–96.
18. Shintomi K, Iwabuchi M, Saeki H, Ura K, Kishimoto T, Ohsumi K. Nucleosome assembly protein-1 is a linker histone chaperone in xenopus eggs. Proc Natl Acad Sci U S A. 2005;102(23):8210–5.
19. Karetsou Z, Sandaltzopoulos R, Frangou-Lazaridis M, Lai CY, Tsolas O, Becker PB, Papamarcaki T. Prothymosin alpha modulates the interaction of histone H1 with chromatin. Nucleic Acids Res. 1998;26(13):3111–8.
20. George EM, Brown DT. Prothymosin alpha is a component of a linker histone chaperone. FEBS Lett. 2010;584(13):2833–6.
21. Hayashihara K, Uchiyama S, Shimamoto S, Kobayashi S, Tomschik M, Wakamatsu H, No D, Sugahara H, Hori N, Noda M, et al. The middle region of an HP1-binding protein, HP1-BP74, associates with linker DNA at the entry/exit site of nucleosomal DNA. J Biol Chem. 2010;285(9):6498–507.
22. Garfinkel BP, Melamed-Book N, Anuka E, Bustin M, Orly J. HP1BP3 is a novel histone H1 related protein with essential roles in viability and growth. Nucleic Acids Res. 2015;43(4):2074–90.
23. Liu H, Liang C, Kollipara RK, Matsui M, Ke X, Jeong BC, Wang Z, Yoo KS, Yadav GP, Kinch LN, et al. HP1BP3, a chromatin retention factor for Co-transcriptional MicroRNA processing. Mol Cell. 2016;63(3):420–32.
24. Abramson J, Adler J, Dunger J, Evans R, Green T, Pritzel A, Ronneberger O, Willmore L, Ballard AJ, Bambrick J, et al. Accurate structure prediction of biomolecular interactions with alphafold 3. Nature. 2024;630(8016):493–500.
25. Zhang Y, Skolnick J. TM-align: a protein structure alignment algorithm based on the TM-score. Nucleic Acids Res. 2005;33(7):2302–9.
26. Lowary PT, Widom J. New DNA sequence rules for high affinity binding to histone octamer and sequence-directed nucleosome positioning. J Mol Biol. 1998;276(1):19–42.
27. Colombo E, Bonetti P, Lazzerini Denchi E, Martinelli P, Zamponi R, Marine JC, Helin K, Falini B, Pelicci PG. Nucleophosmin is required for DNA integrity and p19Arf protein stability. Mol Cell Biol. 2005;25(20):8874–86.
28. Murano K, Okuwaki M, Hisaoka M, Nagata K. Transcription regulation of the rRNA gene by a multifunctional nucleolar protein, B23/nucleophosmin, through its histone chaperone activity. Mol Cell Biol. 2008;28(10):3114–26.
29. Nagata K, Saito S, Okuwaki M, Kawase H, Furuya A, Kusano A, Hanai N, Okuda A, Kikuchi A. Cellular localization and expression of template-activating factor I in different cell types. Exp Cell Res. 1998;240(2):274–81.
30. Dignam JD, Lebovitz RM, Roeder RG. Accurate transcription initiation by RNA polymerase II in a soluble extract from isolated mammalian nuclei. Nucleic Acids Res. 1983;11(5):1475–89.
31. Simpson RT. Structure of the chromatosome, a chromatin particle containing 160 base pairs of DNA and all the histones. Biochemistry. 1978;17(25):5524–31.
32. Misteli T, Gunjan A, Hock R, Bustin M, Brown DT. Dynamic binding of histone H1 to chromatin in living cells. Nature. 2000;408(6814):877–81.

Publisher's note